1D single-shot spontaneous Raman scattering for temperature and multi-species measurements in flame.
Comparison of back-illuminated CCD with BI-EMCCD and ICCD cameras

H. Ajrouche[*, 1], A. Lo[1], P. Vervisch[1], A. Cessou[1]

[1]CORIA UMR 6614 CNRS – Normandie Université, Université et INSA de Rouen, BP 12, 76801 Saint Etienne du Rouvray, France

Abstract

The critical aspect of 1D single-shot Spontaneous Raman Scattering (SRS) experiments in flames is the requirement of high efficiency of the detection system associated with a fast temporal gating. Single-shot SRS measurements in flames are performed either with ICCD or with back-illuminated CCDs associated with a fast shutter. Here, a Pockels cell shutter provides the fast gating for BI-CCD or BI-EMCCD. The purpose of the present paper is to compare the three detectors by quantifying the accuracy and uncertainty of 1D single-shot SRS measurements of temperature, low and high density in near-adiabatic CH_4/air flames. On one hand, the BI-CCD with the PCS is the most efficient detection systems in extreme low light situations for single-shot temperature measurements. On the other hand the BI-EMCCD is the most powerful tool for best detectability of low density species.

Introduction

Validation of theoretical and numerical combustion models has motivated the development of Spontaneous Raman Scattering (SRS) as a multispecies diagnostic [1,2]. Due to its low efficiency, the gas analysis by SRS has been limited for many years to large control volumes and long exposure times. These constraints make the SRS unsuited for the analysis of turbulent flames requiring single-shot measurements with high spatial and temporal resolutions. Therefore, such measurements require on one hand high laser energies, greater than 1J/pulse [3], associated with long pulse duration to avoid optical breakdown [4], and on the other hand very sensitive detectors. Moreover, the weak SRS is usually embedded in the flame emission, thus requiring a detection system not only with high efficiency (high sensitivity, low noise, high dynamic range) but also with a fast temporal gating. Therefore, single-shot SRS measurement in flames are performed either with back-illuminated CCDs (BI-CCD)[5,6] associated with a home-made shutters [7,8] or with ICCD cameras [9–12]. The advantage of each solution is the high sensitivity for BICDD and fast gating for ICCD. Their main drawback is the requirement of developing a shutter for BI-CCD and the high shot-noise for ICCD [13,14] . The recent development in the field of signal detection is the electron multiplying CCD camera BI-EMCCD, which combines extremely high quantum efficiency (QE), when back-illuminated (BI-EMCCD), with the ability to eliminate the readout noise detection limit [15–17] but keeps the need for a fast shutter.

We have previously proposed a new experimental set-up for 1D single-shot measurements of temperature and concentration of major species by SRS [18,19], where the ability of a Pockels cell shutter (PCS) to enhance the signal-to-noise ratio (SNR) has been demonstrated [20]. The applicability of PCS as optical gating for BI-CCD and BI-EMCCD makes these cameras suitable for Raman measurements in flame [17].

Specific objectives

In the present work, we studied the potential applicability and the limitation of the three detector types for instantaneous 1D Raman measurements of temperature and species concentrations in flame. The ability to measure single-shot scalar values accurately in flames is assessed by comparing the BI-CCD, BI-EMCCD and ICCD detection systems. First, a comparative analysis of the performances of these devices has been performed, principally to illustrate the effect of each detector on fundamental SNR considerations. Second, thermometry by SRS, which offers the advantage of not requiring reference temperature, has been proposed in previous work [18,19]. The accuracy and uncertainty of temperature in near-adiabatic CH_4/air flames according to the detector used are analyzed and compared to adiabatic 1D freely propagating laminar flames modeling. Third, 1D single-shot density measurements of the 3 detectors are compared for N_2 concentration quantified when crossing the flame front and for density corresponding to signal close to the detectability limit by probing CO in a near-stoichiometric rich premixed flame.

Experimental setup

The experimental set-up has been described in detail elsewhere [18,20] and only a short summary will be given here. Fig. 1 shows the layout of the SRS set-up. The laser source consists in a Nd:YAG laser (Agilite Continuum) operating at 10 Hz providing about 1.2 J with top-hat pulse with a long pulse duration adjustable from 200 ns till 1 µs. A long pulse duration provides a large energy deposit suitable for single-shot SRS [3], with good spatial resolution and without optical

* Corresponding author: hassan.ajrouche@coria.fr
Proceedings of the European Combustion Meeting 2015

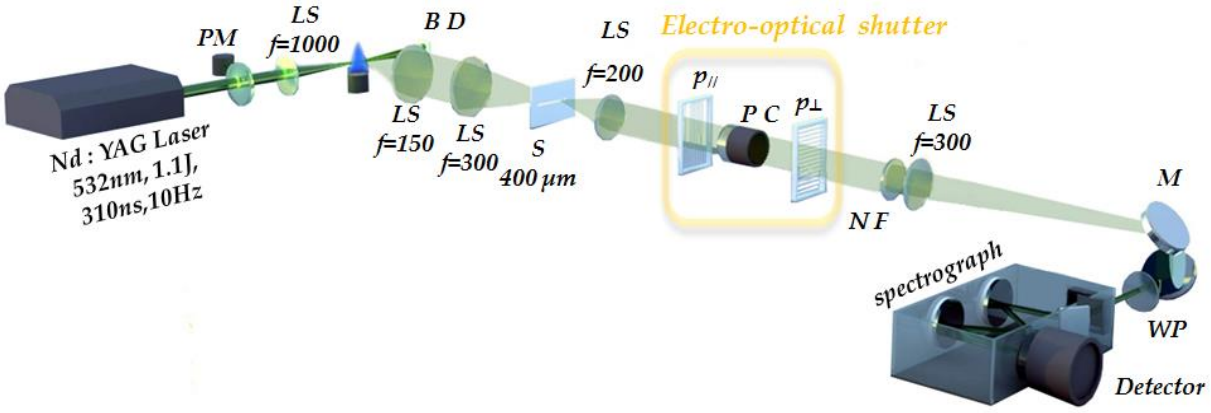

Fig. 1: Overview of the experimental set-up: S, slit; LS, Lens (AR coated @400-700nm) PC, Pockels Cell; P, Polarizer; BD, beam dump; PM, Power meter; NF, Notch filter (532 nm, FWHM 20 nm); WP, Waveplate (λ/2, AR coated @400-700nm)

breakdown occurring when instantaneous and local irradiance is greater than a threshold value of 34 GW/cm^2 [4]. The pulse duration used in this study is 310 ns. The laser beam is focused using a convergent lens with a 1 m focal-length providing a probe volume of 170 µm- thick (1/e^2). The SRS light is collected at right angle to the laser beam with a large solid angle (f/2) using two telescopes composed of achromatic lenses. The scattered light at the laser wavelength is rejected by a notch filter (HNPF-18702, Kaiser Optical System, OD=6, FWHM 20 nm, transmission efficiency in passbands >80%) placed in the second collimated part of the optical collection system. Then, a periscope is used to rotate the image of the laser beam parallel to the entrance slit of the spectrograph.

In this study, three types of camera are compared with different quantum efficiency (QE) and noise factor (NF), which originates from the amplification process, defined as: the ratio of the output noise of the amplifier to the product of the multiplication gain by the input noise. An ideal amplifier will therefore have a noise factor of 1. The consequence of the stochastic nature of the gain in both BI-EMCCDs and ICCDs is a fundamental parameter affecting the SNR.

The ICCD detector used is a 16 bit CCD camera equipped with a GenIII intensifier (PI-MAX UNIGEN, Princeton Instruments, 512 x 512pixels, pixel size 23µm, readout rate of 1 MHz). The maximal QE provided by this device is 38% between 400 and 700 nm and its NF ranges between 1.6 and 3.5 [21,22]. The image intensifier was operated in gated mode with a gate width of 500 ns, suitable to suppress non-laser-induced emissions, such as flame luminosity.

The back-illuminated CCD camera is a full-frame CCD (Pixis 400B, Princeton Instruments, 1340x400 pixels, pixel size 20 µm, NF=1). This camera offers approximately 94 % of QE with 16-bits of dynamic range and readout noise (<13e-). Different analog-to-digital converters (ADC) are available as 1-2 MHz or 100 KHz. Because the readout noise of CCD arrays increases with the readout rate, the 100 KHz ADC is chosen to enhance the SNR for Raman active species.

The last camera is a back-illuminated electron-multiplying CCD camera (BI-EMCCD) (ProEM, Princeton Instruments, 1600x200pixels, pixel size 16 µm, 94% of QE). The selected EM gain setting was approximately (x200) and was sufficient to make the readout noise negligible. The readout rate used in this study is 1MHz. A fast electro-optical shutter is used for SRS measurements in flame with the 2 non-intensified detectors (BI-CCD or BI-EMCCD). The PCS consists of a large aperture Pockels cell (LAP-50, KD*P, 50 mm aperture, Quantum Technology) between 2 crossed polarizers (19WG-50, Quantum Technology), The two crossed wire-grid polarizers have high transmission (85% of the polarized incident light for each polarizer) leading to PCS transmission of about 72% of the Raman signal [18–20]. With the PCS switched on, the flame emission is integrated on a small time interval (500 ns), and its contribution on the spectra becomes negligible. After the PCS, an achromatic half-wave plate (AHWP10M-600, THORLABS) is placed in front of the spectrograph in order to fit collected SRS signal to the polarization of the grating.

Results and Discussion

Single-shot SRS temperature and multispecies measurements from BI-CCD, BI-EMCCD and ICCD are compared by measurements in a premixed laminar flame, stabilized downstream a Bunsen burner fed with a methane-air mixture with equivalence ratios of Φ=1 and 1.4. The measurements are compared to modeling calculation of 1D freely propagating laminar flame by the COSILAB [23] software, using the GRI-Mech 3.0 chemical mechanism [24]. Since the laser beam does not cross the flame front perpendicularly, the experimental profiles are corrected from the angle effect assuming that the tangential temperature gradients are negligible at the height probed, far from the flame tip and burner lip.

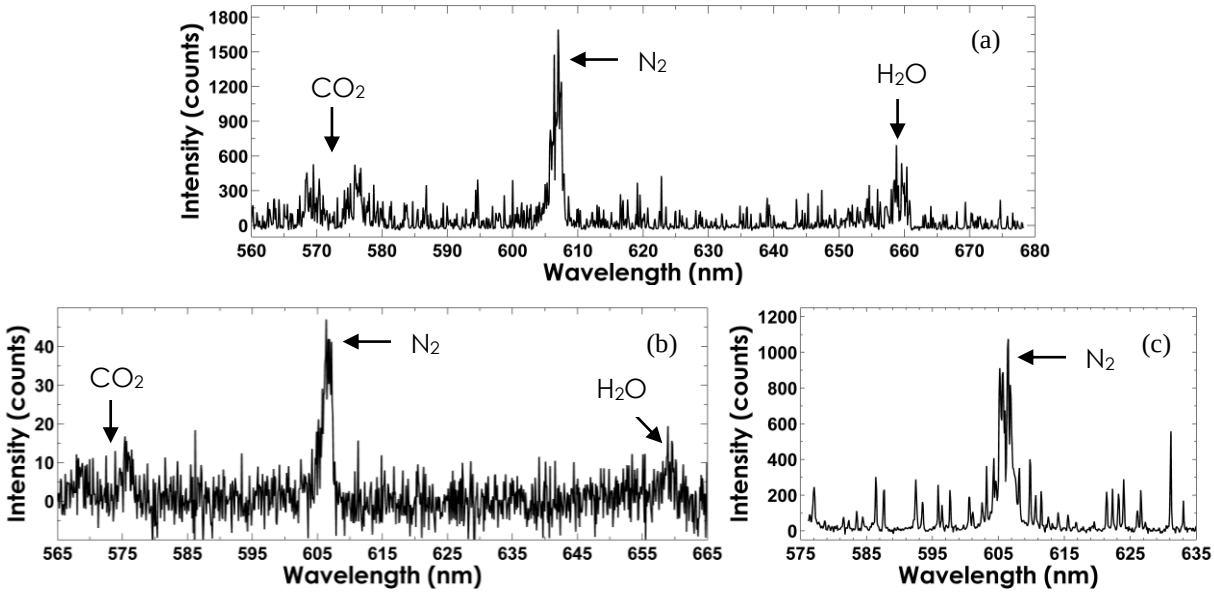

Fig. 2: Samples of single shot Raman spectra acquired in stoichiometric methane-air flame with 160 µm spatial resolution (2130 K) using (a) BI-EMCCD (b) BI-CCD (c) ICCD.

In first approximation the stretch effect on the temperature and species profiles are neglected. This assumption will be discussed afterwards. Most of the measurements are performed at Φ=1, for which the adiabatic temperature determined by modeling is 2136 K. The Φ=1.4 flame is used to assess the cameras for measuring low level of concentrations, especially in probing CO which is a species difficult to probe by SRS in flame [25]. The burner is mounted on x-y-z translation stages with an accuracy of 100 µm. The SRS measurements are performed at two heights above the burner (8 and 24 mm). The SRS radial profiles performed at height of 8 mm above the burner exit, labeled FG, offer measurements in various conditions: fresh mixture near the centerline, homogeneous burnt gas at the periphery, and sharp temperature and composition gradient for the intermediate radii, when crossing the preheat and reaction zone. At this height the flame front is stable. The second height, labeled (BG), is located 24 mm above the burner exit in the burnt gas areas of the flame, in a region of homogeneous temperature and composition, close to equilibrium conditions.

The possibility of measuring single-shot temperature from SRS has been demonstrated in previous work using BI-CCD camera with a PCS shutter [18–20]. Here the single-shot temperature measurements from BI-CCD, BI-EMCCD and ICCD are compared and analyzed in terms of uncertainty and accuracy. The temperature is determined by simulating the vibration-rotation spectra of N_2 by theoretical spectra. These spectra are calculated and convoluted with the in-situ instrumental functions [19,26]. The SNR values obtained from single-shot spectra are defined as the ratio of peak Raman intensity of fitted spectra, considered as the "true" signal value, divided by the root-mean-square (rms) fluctuations of the difference between experimental and fitted spectra calculated in the wavelength range of the SRS signal.

Fig. 2 shows an example of single-shot Raman spectra with a spatial resolution of 160 µm, obtained on the axis of the collection system at BG for the three detectors, illustrating their different nature of noise. The two spectra acquired with the BI-EMCCD and BI-CCD show the SRS signal of the rovibrational bands of CO_2, N_2 and H_2O (Fig. 2 a, b). Fig. 2 (c) shows that the single-shot spectra obtained with BI-CCD and BI-EMCCD are weakly noisy, SNR of 9.92 and 8.89 respectively, and very reproducible from one shot to another. While instantaneous spectra acquired with ICCD is altered by shot noise, and varies from one shot to another. Here, SNR of 5.84 much lower than for the 2 other camera is noticed.

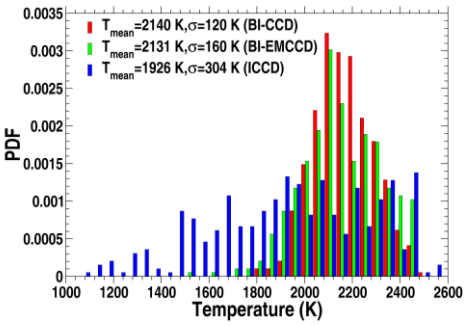

Fig. 3: PDF of Raman Temperature measurements with the 3 detectors at BG with 160µm. spatial resolution.

Fig. 3 shows temperature PDF from stoichiometric methane-air flame, measured with the 3 detectors at BG. The average temperatures measured are 2140K, 2131K for BI-EMCCD and BI-CCD respectively. They are very close to the temperature calculated by adiabatic flame modeling COSILAB (2136K) [23] and demonstrate that the combustion can be considered almost adiabatic in this area.

In the following, the COSILAB modeling will be considered to provide the reference data (temperature and major species) of the flame. The comparison of temperature accuracy between the BI-EMCCD and BI-CCD detectors highlights their ability to provide accurate temperature measurements with an error smaller than 1% and shows the reliability and the reproducibility of experimental procedure proposed. Temperature fluctuations are almost equal for these two detectors with slight higher uncertainties obtained with BI-EMCCD (160K) than those with BI-CCD (120K). We can point out that when BI-EMCCD gain is set to 1 similar fluctuation levels (124K) to those with the standard BI-CCD are obtained. For ICCD, the temperature measurements are clearly affected by the higher NF of this device degrading the SNR from 9.92 with BI-CCD to 5.84 with ICCD and resulting in an average temperature of 1926K clearly smaller than the calculated temperature (2136K) and very high uncertainties (340K). This is due to the decrease in the spectral resolution of the vibrational bands because of the higher pixel size and the higher shot noise of this detector.

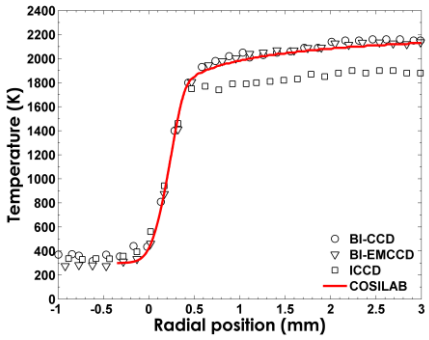

Fig. 4: 400-shot averaged radial profiles of temperature from stoichiometric methane-air flame, measured by the three detectors at FG compared to temperature values calculated by COSILAB.

Fig. 4 compares averaged single-shot temperature to the calculated profile for the three detectors. The profiles obtained from both BI-CCD and the BI-EMCCD at 160 µm spatial resolution are in agreement with the COSILAB calculations. The profiles fit well with the modeling with a maximum shift at the inflexion point of 50 K for BI-EMCCD, which is reduced to 24 K for BI-CCD. This agreement shows that the stretch rate does not affect the temperature profile in the present work.

For ICCD, the temperature profile is significantly affected by the higher shot noise, which degrades the fitted spectra and leads to an underestimation of the temperature on the plateau due to the shot-to-shot signal variation. However, the averaged experimental temperature values obtained from mean spectra acquired with ICCD are more accurate. Temperature of 2100 K is observed on the temperature plateau at BG, which implies temperature measurement in our configuration can be performed with ICCD only for average spectra where the noise effect is reduced.

The 3 detectors are now compared by measuring species concentrations firstly with high concentration levels by probing N_2 in the stoichiometric flame and then with low concentration levels by probing CO in the Φ=1.4 flame. Density is determined using the area of theoretical spectra and the fitted temperature. The accuracy of N_2 density measurement is first assessed at BG. The measured densities are $2.483x10^{18}\pm 1.8x10^{17}cm^{-3}$, $2.623x10^{18}\pm3.812x10^{17}cm^{-3}$ and $3.95x10^{18} \pm 1.04x10^{18}cm^{-3}$ for BI-CCD, BI-EMCCD and ICCD respectively. Density values obtained with BI-CCD are very close to the density calculated by adiabatic flame modeling COSILAB ($2.48x10^{18}$ cm^{-3}). Density obtained with BI-EMCCD is slightly underestimated due to the higher uncertainty of temperature with this detector. If the modeled temperature from COSILAB is used instead of the instantaneous temperature measured, the density value is $2.36\ x10^{18} \pm 2.66x10^{17}cm^{-3}$, showing that for this camera the uncertainty is due to the temperature uncertainty measured from SRS.

For ICCD, the underestimation and uncertainties of density measurements are high. These results suggest that temperature is very important parameter which affects density measurements. When the modeled temperature is used, the results show more accurate density values $2.56x10^{18}$ cm^{-3} instead of $3.95x10^{18}$ cm^{-3} and lower uncertainty values which are significantly reduced from ($1.04x10^{18}$ cm^{-3}) with temperature measured by ICCD to ($4.48x10^{17}cm^{-3}$) with temperature provided by simulation. In this case, if ICCD detector is used for density measurements, temperature should be measured by an independent simultaneous measurement, like Rayleigh scattering or SRS with BI-CCD associated with a fast shutter.

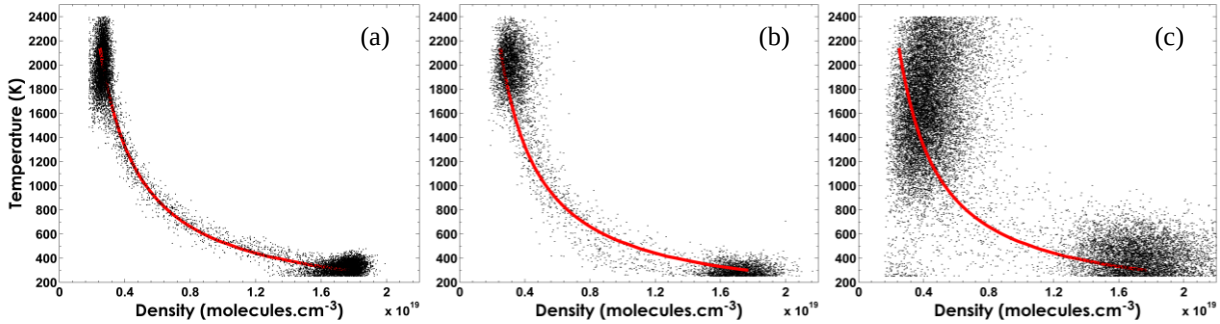

Fig. 5: Scatter plots of instantaneous measurements of temperature versus density of N_2 at front flame for different detectors: BI-CCD (a) BI-EMCCD (b) and ICCD (c) compared to laminar flame calculation (solid red curve)

Scatter plots of instantaneous temperature measurements versus density of N_2 with 160 µm spatial resolution measured at FG when crossing the front flame are plotted for different cameras in Fig. 5 superimposed to the modeled profile. The BI-CCD measurements reproduced well the hyperbolic behavior. The dispersion of 9.5% from either side of the modeled curve is acceptable especially if we consider the small probe volume. This dispersion is reduced to 6.7 % for a probe volume of 300µm. The density measurements performed with BI-EMCCD present approximately similar results to those obtained with BI-CCD with higher dispersion of the values due to the higher uncertainties of temperature measurements performed with BI-EMCDD (Fig. 5 (b)).

The scatter plot dispersion of N_2 density measurements performed with ICCD is very broad due to the cumulated uncertainty of density and temperature measurements (Fig. 5 (c)). The question arises whether the temperature is the cause of the loss of the precision on the density measurements characterized by the increase in density uncertainties. The results discussed in the previous paragraph show that temperature is the key parameter which affects density measurements and that for ICCD camera the temperature measurements must be performed by another method.

Fig. 6 presents an example of single shot SRS spectra of N_2 and CO acquired in burnt gases (160 µm spatial resolution) recorded with each camera, with their respective calculated fit. For illustration, the spectra were chosen among the 400 single-shot spectra for the temperature corresponding to the COSILAB temperature in burnt gases at Φ=1.4 (T=1940 K). In Fig. 6 (a) acquired from BI-CCD, the CO peak of few counts (~5) is difficult to distinguish with a SNR value of 0.92 (*Table 1*). The small peak value of CO obtained with BI-CCD can be embedded for some single shot spectra in the background signal and therefore information about CO will be lost. As for Fig. 2 (a) above, the improvement in BI-EMCCD signal quality is immediately noticeable in Fig. 6 (b). Therefore, the use of BI-EMCCD increases the detectability of CO peak to 350 counts with a SNR of approximately 1.5. BI-EMCCD can detect very low CO signal. For ICCD, the high shot noise decreases drastically the SNR of the CO peak to 0.84, and makes the detectability of the peak very low. We have to remember here that CO density measurement by SRS is not usual due to the low level of signal and that this issue is enhanced here by the small probe volume (160 µm).

Detector	BI-CCD	BI-EMCCD	ICCD
SNR (160µm)	0.92	1.49	0.84
Density x10^{17}cm^{-3}(160µm)	3.02	2.89	3.35
Uncertainties (x10^{17}cm^{-3})	1.54	1.03	2.22
Accuracy (%)	3.7	0.6	15
Density x10^{17}cm^{-3}(300µm)	2.92		3.01
Uncertainties (x10^{17}cm^{-3})	1.11		1.69
Accuracy (%)	0.3		3.4

Table 1: Table of representative SNR of detectability, measured density of CO, accuracy and uncertainties obtained in methane-air premixed flame (Φ=1.4) at a homogenous temperature zone (z=24 mm) for different detector.

The COSILAB value of CO density is 2.91x10^{17} cm^{-3} for Φ=1.4 methane-air premixed flame. Despite the acceptable accuracy of density measurements of CO performed with BI-CCD for 160 µm spatial resolution (3.02x10^{17}cm^{-3}), the uncertainties are high (50%) compared to the values obtained with BI-EMCCD (35%). These high values are due to the low level of detectability of these detectors for low signal in the hot gases. Again ICCD presents a shift in the average value from COSILAB value and high uncertainties (66%). The use of an alternative for temperature measurement, like Rayleigh scattering, is essential to perform low concentration species with ICCD detector.

For BI-EMCCD, density values of CO are very close to the density calculated by adiabatic flame modeling, showing the benefit provided by the electron multiplication gain. To compensate the loss in detectability for BI-CCD, SNR improvement has to be achieved either by enlarging the probe volume, increasing the laser energy or by increasing the efficiency of the collection system. When the length of the probed volume is increased to 300 µm leading to an improvement of about 44% in SNR. An improvement in accuracy is obtained from both BI-CCD and the BI-EMCCD and a reduction in uncertainties by a factor of about 1.38 appears (*Table 1*).

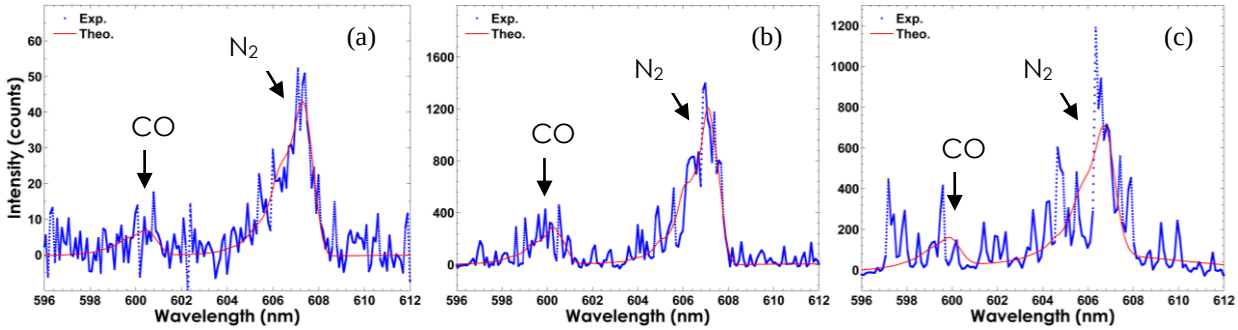

Fig. 6: Example of single shot N_2 and CO Raman intensities in premixed methane-air flame Φ=1.4 (blue points). The solid red curve is the theoretical best-fit obtained for BI-CCD (a) BI-EMCCD (b) and ICCD (c)

Conclusions

In flames, where the SRS signal is embedded in continuous background radiation, different types of cameras can be used for signal detection: BI-CCD, BI-EMCCD and ICCD. BI-CCD and BI-EMCCD offer advantages for SRS measurements, due to their high quantum efficiency and limited shot-noise. However, measurements in flame with these types of cameras require the use of a fast shutter device. Here a Pockels cell shutter PCS is used as optical gating for BI-CCD and BI-EMCCD, in order to assess accuracy and uncertainties of SRS measurements in flames and to compare their performances to those of ICCD cameras. Results obtained with BI-CCD and BI-EMCCD for temperature, temperature gradient, and high density are in good agreement with laminar flame calculations. Fluctuations in the measured temperature with BI-CCD and BI-EMCCD for high spatial resolution (160 µm) are below 7% in burnt gases. Temperature measurements performed with ICCD camera are not so accurate and present high uncertainties due to the high shot noise. The measurements with ICCD are limited to larger probe volume and density measurements must be associated to another temperature measurement than SRS proposed here, as Rayleigh scattering for instance.

PCS offers time gates comparable to ICCD, and it makes on one hand the BI-CCD, the most efficient detection systems for single-shot temperature measurements but for single-shot density measurements with low detectability the measurements are readout noise limited. On the other hand, the BI-EMCCD is the powerful tool for best detectability of low concentration species such as CO. The powerful improvement for BI-EMCDD is obtained because this detector removes the readout noise detection limit by applying a low-noise gain process, to enhance the signal above the noise background. This study opens prospects for the analysis of turbulent reacting flows by simultaneous 1D measurements of temperature and concentrations of major species.

Acknowledgements

This work was supported by the Haute-Normandie Region for the PhD fellowship of H. Ajrouche.

References

[1] R.S. Barlow, Proc. Combust. Inst. 31 (2007) 49–75. doi:10.1016/j.proci.2006.08.122.
[2] K.N. Gabet, N. Jiang, W.R. Lempert, J.A. Sutton, Appl. Phys. B. 101 (2010) 1–5. doi:10.1007/s00340-010-4208-2.
[3] W. Meier, O. Keck, Meas. Sci. Technol. 13 (2002) 741–749.
[4] G. Cléon, D. Stepowski, A. Cessou, Opt. Lett. 32 (2007) 3290–3292. http://www.ncbi.nlm.nih.gov/pubmed/18026283.
[5] J.M. Fernández, a. Punge, G. Tejeda, S. Montero, J. Raman Spectrosc. 37 (2006) 175–182. doi:10.1002/jrs.1462.
[6] F. Vestin, M. Afzelius, C. Brackmann, P.-E. Bengtsson, Proc. Combust. Inst. 30 (2005) 1673–1680. doi:10.1016/j.proci.2004.08.043.
[7] J. Kojima, Q.-V. Nguyen, AIAA J. 46 (2008) 3116–3127. doi:10.2514/1.37433.
[8] P.C. Miles, R.S. Barlow, Meas. Sci. Technol. 11 (2000) 392–397. doi:10.1088/0957-0233/11/4/308.
[9] D. Geyer, A. Kempf, A. Dreizler, J. Janicka, Combust. Flame. 143 (2005) 524–548. doi:10.1016/j.combustflame.2005.08.032.
[10] T. Cheng, C. Wu, C. Chen, Y. Li, Y. Chao, T. Yuan, et al., Combust. Flame. 146 (2006) 268–282. doi:10.1016/j.combustflame.2006.03.005.
[11] M.S. D. Müllera, W. Triebela, A. Bochmanna, G. Schmidla, D. Eckardta, A. Burkerta, J. Röperb, SPIE VOL. 5191 Opt. Diagnostics Fluids, Solids, Combust. II. (2003) 1–9.
[12] H. Zhao, S. Zhang, J. Phys. Conf. Ser. Third Int. Conf. Opt. Laser Diagnostics. 85 (2007) 012006. doi:10.1088/1742-6596/85/1/012006.
[13] K.C. Utsav, P.L. Varghese, Appl. Opt. 52 (2013) 5007–21. http://www.ncbi.nlm.nih.gov/pubmed/23852217.
[14] L. Wehr, P. Kutne, W. Meier, J. Becker, Proc. Eur. Combust. Meet. 2005. (2005) 1–6.
[15] M.A. Gregor, A. Dreizler, Meas. Sci. Technol. 20 (2009) 065402. doi:10.1088/0957-0233/20/6/065402.
[16] A.C. Bayeh, PhD Thesis, Univ. Texas Austin, United States Am. (2013) 1–119.
[17] C.N. Dennis, C.D. Slabaugh, I.G. Boxx, W. Meier, R.P. Lucht, Proc. Combust. Inst. (2014). doi:10.1016/j.proci.2014.06.063.
[18] H. Ajrouche, A. Lo, P. Vervisch, A. Cessou, 17th Int. Symp. Appl. Laser Tech. to Fluid Mech. Lisbon, Port. (2014) 1–17. doi:978-989-98777-8-8.
[19] H. Ajrouche, A. Lo, P. Vervisch, A. Cessou, 14éme Congrès Francoph. Tech. Laser MARSEILLE, 15–19 Sept. 2014. (2014) 1–9.
[20] A. Lo, H. Ajrouche, P. Vervisch, A. Cessou, Proc. Eur. Combust. Meet. (2013) 1–7.
[21] M.S. Robbins, S. Member, B.J. Hadwen, IEEE Trans. Electron Devices. 50 (2003) 1227–1232.
[22] D. Dussault, P. Hoess, SPIE. 5563 (2004) 195–204. doi:10.1117/12.561839.
[23] COSILAB, Combust. Simul. Lab. (2007).
[24] G. Smith, D. Golden, M. Frenklach, T. Bowman, N. Moriarty, B. Eiteneer, et al., <http://www.combustion.berkeley.edu/gri_mech/>. (n.d.).
[25] R. Barlow, G. Wang, P. Anselmofilho, M. Sweeney, S. Hochgreb, Proc. Combust. Inst. 32 (2009) 945–953. doi:10.1016/j.proci.2008.06.070.
[26] A. Lo, G. Cléon, P. Vervisch, A. Cessou, Appl. Phys. B Lasers Opt. 107 (2012) 229–242. doi:10.1007/s00340-012-4874-3.